

# Water-Soluble Multiwalled Carbon Nanotubes Functionalized with Sulfonated Polyaniline

Hui Zhang, Hong X. Li, and Hui M. Cheng\*

Shenyang National Laboratory for Materials Science, Institute of Metal Research, Chinese Academy of Sciences, 72 Wenhua Road, Shenyang 110016, China

Received: January 11, 2006; In Final Form: March 17, 2006

Multiwalled carbon nanotubes (MWNTs) functionalized with a water-soluble conducting polymer, sulfonated polyaniline (SPAN), were prepared by in situ polymerization of aniline followed by sulfonation with chlorosulfonic acid in an inert solvent and by hydrolysis in water. Electron microscopy, laser Raman spectroscopy, X-ray photoelectron spectroscopy, and UV–vis absorption spectroscopy were employed to characterize the morphology and chemical structure of the resulting product. The results show that the quinonoid structure of SPAN preferentially interacts with the nanotubes and is stabilized by strong  $\pi$ – $\pi$  interaction between two components. The structure of MWNTs was not perturbed by the incorporation of SPAN, since the  $\pi$ – $\pi$  interaction between MWNTs and SPAN is much weaker in comparison to that of the carbon covalent bond. The SPAN functionalized MWNTs are highly dispersible in water, thus opening new possibilities for their prospective technological applications.

## 1. Introduction

Carbon nanotubes (CNTs) possessing unique structure and properties are attractive building blocks for novel materials and devices of important practical interest.<sup>1</sup> However, the insolubility or poor dispersibility of pristine CNTs in common solvents poses a serious obstacle to their further development. Various attempts have been made to obtain homogeneous CNT dispersions in both aqueous and organic media.<sup>2,3</sup> Among those approaches, chemical modification of side walls, defect sites, and open ends are often found to result in changes of the structural, mechanical, and electronic properties of CNTs.<sup>4</sup> Noncovalent methods based mainly on physical adsorption of surfactants or polymers were then developed,<sup>5,6</sup> showing the advantage of leaving the electronic structure of CNTs intact. However, noncovalent functionalization is a more effective way to disperse single-walled carbon nanotubes (SWNTs) than multiwalled carbon nanotubes (MWNTs), since the polymer chain length and surface coverage necessary for inducing steric repulsion in MWNT dispersions are much higher than those required for dispersion of SWNTs.<sup>7</sup> On the other hand, to obtain CNT dispersions by using high concentrations of surfactants or polymers will bring about inconvenience in their further processing such as making composite materials. Therefore, an effective noncovalent side wall functionalization technique for MWNTs is highly desirable from the viewpoint of both fundamental study and technical application.

Polyaniline (PANI) is an important conjugated conducting polymer showing good environmental stability, high electrical conductivity, and unique redox properties. Recently, the studies on CNT/PANI composites revealed good interactions between the components especially when polymerization took place in the presence of CNTs.<sup>8</sup> However, the resulting composites are insoluble in conventional solvents and difficult to process, greatly hindering their practical applications. The attempts at solubilizing CNT/PANI composites in organic solvents have relied on PANI derivatives (e.g., polyanisidine<sup>9</sup> and emeraldine

base<sup>10</sup>) to wrap CNTs. The most successful approach toward soluble conducting PANI is the synthesis of sulfonated polyaniline (SPAN), which has potential applications in electronic devices.<sup>11</sup> The combination of CNTs and SPAN into composite materials will broaden the application of CNTs and SPAN by tailoring their solubility properties. For example, SWNT/poly(*m*-aminobenzene sulfonic acid) composite produced by covalent functionalization has shown improved sensor performance for detection of NH<sub>3</sub>.<sup>12</sup>

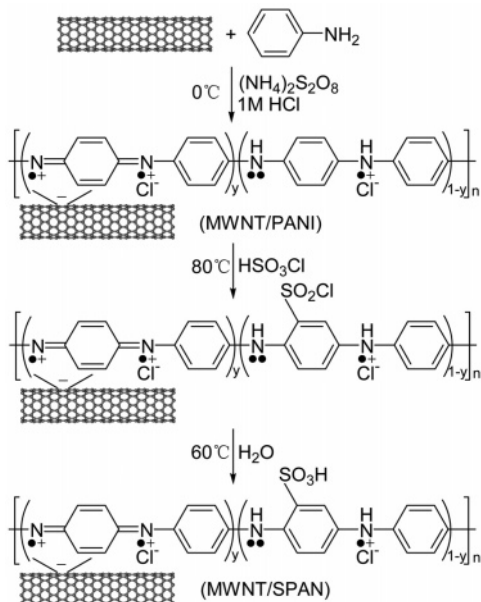
We report here a facile approach to noncovalently functionalize graphitized MWNTs, which exhibit fine crystalline structure and high conductivity, with the water-soluble conducting polymer of SPAN. The functionalization was based on the in situ polymerization of aniline and MWNTs followed by sulfonation with chlorosulfonic acid in an inert solvent and by hydrolysis in water. The lengths and surface structure of MWNTs were not perturbed with the incorporation of SPAN. The SPAN functionalized MWNTs (MWNT/SPAN composite) are highly soluble in water, thus opening many new possibilities for their prospective technological applications.

## 2. Experimental Section

**Synthesis of the MWNT/SPAN Composite.** The MWNTs employed were produced by a chemical vapor deposition method<sup>13</sup> and were graphitized at 2600 °C, having micrometer-lengths and diameters of 20–50 nm. The purity of MWNTs is higher than 95%. Scheme 1 shows the detailed synthesis route of the MWNT/SPAN composite. For the fabrication of the MWNT/PANI composite, an in situ polymerization of aniline in the presence of 20 wt % MWNTs was applied.<sup>8b</sup> The resulting MWNT/PANI composite was filtered, washed, and then dried in a vacuum overnight. Dried MWNT/PANI powder (2 g) was dispersed in 200 mL of 1,2-dichloroethane (DCE) and stirred at 80 °C. The chlorosulfonic acid (3.5 g) diluted with 10 mL of DCE was added dropwise for 30 min, and then the reaction mixture was held for 4 h. The produced chlorosulfonated MWNT/PANI was separated by filtration, immersed in water, and heated for 4 h at 60 °C to promote its hydrolysis. In this

\* Address correspondence to this author. E-mail: cheng@imr.ac.cn.

### SCHEME 1: Synthesis Route of the MWNT/SPAN Composite



way, the PANI component was transformed into SPAN.<sup>14</sup> The MWNT/SPAN was separated by filtration and washed with water. Green filtrate obtained at this stage was collected for observation. The filter cake (MWNT/SPAN) was stirred in water for 24 h at room temperature and rested for more than 2 days to settle insoluble particles, and then the MWNT/SPAN sample was carefully separated by filtration from the supernatant liquid.

**Characterization.** The products were studied by scanning electron microscopy (SEM) and transmission electron microscopy (TEM) observations (JEOL-2010, 200kV). The samples for SEM and TEM measurements were prepared by placing a few drops of MWNT or MWNT/PANI ethanol suspension, or MWNT/SPAN water suspension, on copper supports and carbon mesh-coated copper grids, respectively. The Raman measurements were carried out with a Jobin Yvon Lab Ram Raman microscope at an excitation laser wavelength of 632.8 nm. X-ray photoelectron spectroscopy (XPS) measurements were carried out with a PHI5300 XPS spectrometer with a Mg K $\alpha$  X-ray source (1253.6 eV). All core-level spectra were referenced to the C1s neutral carbon peak at 284.6 eV and were deconvoluted into Gaussian component peaks. UV-vis absorption measurements were performed with a SHIMAZU 2550 UV-vis spectrophotometer.

### 3. Results and Discussion

Unlike the pristine MWNTs (Figure 1a), the synthesized MWNT/SPAN composite was completely soluble in water and resulted in a stable black suspension for at least 3 months (Figure 1b). The solubility of MWNT in water was determined according to a method reported in the literature:<sup>15</sup> the MWNT/SPAN sample was added to 10 mL of deionized water and stirred vigorously until the solution was saturated. The resulting suspension was allowed to stand overnight. The dark-colored, clear supernatant of accurate volume was carefully transferred into another vessel and water was removed by vacuum drying to recover the MWNT/SPAN composite. The weight of the recovered MWNT/SPAN composite was determined and the MWNT-equivalent aqueous solubility can be estimated since the MWNT content in the soluble composite (about 85 wt %) was known by thermogravimetric analyses (TGA) results which

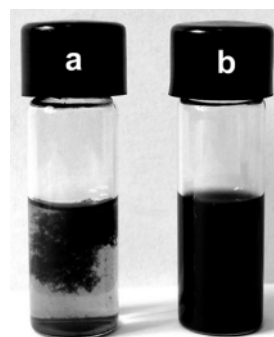


**Figure 1.** Stability of (a) pristine MWNTs in water for 10 min and (b) MWNT/SPAN in water for 3 months.

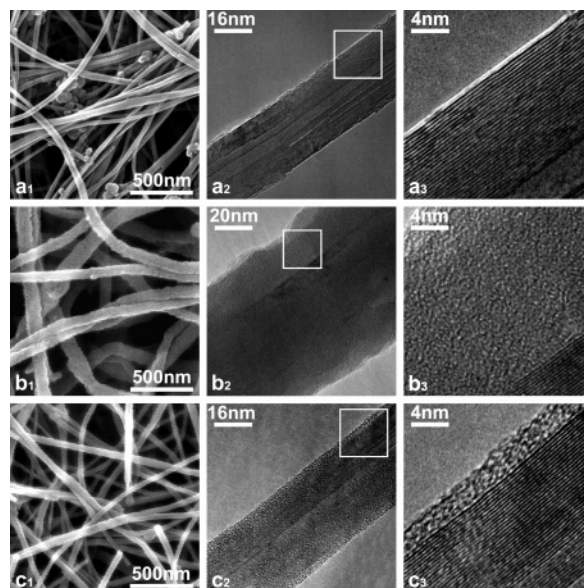


**Figure 2.** SEM (1) and TEM (2, 3) images of (a) MWNTs, (b) MWNT/PANI, and (c) MWNT/SPAN.

are shown in the Supporting Information. The solubility of MWNTs in water was measured to be about 1.9 mg/mL.

Electron microscopy is an effective technique for studying polymer-wrapped CNTs, as both components can be identified in the images. Figure 2a shows the densely entangled pristine MWNTs with a well-graphitized structure. In contrast, isolated MWNTs are observed after surface modification (Figure 2b,c), indicating that the interaction between polymer molecules and CNTs overcomes the van der Waals interaction between CNTs, which generally results in CNT aggregates or bundles. It is worthy to note that the lengths of the MWNTs were not changed, though cutting often occurred in covalent functionalization or prolonged sonication.<sup>3f</sup> Moreover, compared to the thick PANI layer on the MWNT/PAN (Figure 2b<sub>3</sub>), the surface of the MWNT/SPAN is covered by a uniform and thin layer of amorphous SPAN polymer (Figure 2c<sub>3</sub>) and is apparently the reason accounting for the good stability of the MWNT/SPAN dispersion. The thickness of the SPAN polymer layer on the MWNT surface is about 2 nm as observed from the TEM image. This indicates that the outer layer of SPAN, which interacted weakly with MWNTs, was removed during the hydrolysis process and the following filtration, leaving the inner layer of SPAN tightly attached onto the nanotube surface. In this way, MWNTs can be stabilized in water with a low content of polymer (15 wt % determined by TGA).

Water-soluble MWNT/SPAN composite was studied with spectroscopic methods to characterize the interactions between

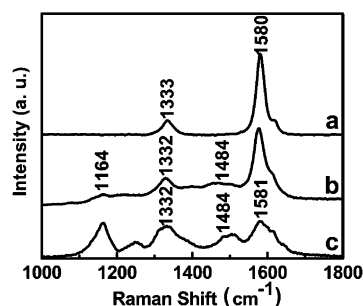


**Figure 3.** Raman spectra of (a) MWNT, (b) MWNT/SPAN, and (c) MWNT/PANI.

MWNTs and the adsorbate molecules. The Raman spectroscopy technique is sensitive to the electronic structure and vibrational properties of both CNTs and conducting polymers.<sup>16</sup> Figure 3 shows the Raman spectra of MWNTs and the MWNT/SPAN and MWNT/PANI composites at a laser energy of 1.96 eV (632.8 nm). The Raman spectrum of MWNTs (Figure 3a) exhibits three normal bands: the disorder-induced D-band at 1333  $\text{cm}^{-1}$ , the G-band at 1580  $\text{cm}^{-1}$ , and a shoulder around 1620  $\text{cm}^{-1}$  assigned to the D'-band. The spectrum of the MWNT/PANI composite (Figure 3c) shows the typical bands of the coated polymer on MWNTs, which is in good agreement with the previously reported results:<sup>17</sup> C-H bending of the quinonoid/benzenoid ring at 1164  $\text{cm}^{-1}$ , C-N<sup>+</sup> stretching at 1332  $\text{cm}^{-1}$ , C-C stretching of the benzenoid ring at 1581  $\text{cm}^{-1}$ , and the C=N stretching corresponding to the quinonoid ring at 1484  $\text{cm}^{-1}$ . The spectrum of the MWNT/SPAN composite (Figure 3b) is almost identical with that of the MWNT/PANI composite except for the weaker intensity of each band due to the relatively low content of polymer in the composite. Here, two points should be noted: (1) There is a remarkable decrease in relative intensity of the C-H bending at 1164  $\text{cm}^{-1}$  with respect to C=N stretching at 1484  $\text{cm}^{-1}$  when compared with that of the MWNT/PANI composite, indicative of the presence of sulfonated rings in the MWNT/SPAN composite, and (2) the intensity of the D-band of the MWNT/SPAN composite increases slightly with respect to that of the MWNTs, which is mainly due to the contribution from SPAN at 1332  $\text{cm}^{-1}$ , consistent with noncovalent modification.

Understanding the structure of the polymer would be instructive and useful in discussing the interactions between the polymer and MWNTs. PANI has the general formula of  $[(\text{-B-NH-B-NH-})_y(\text{-B-N=Q=N-})_{1-y}]_n$ , in which B and Q denote  $\text{C}_6\text{H}_4$  rings in the benzenoid and quinonoid units, respectively. XPS provides a useful tool for the quantitative analysis of the intrinsic redox state of PANI and its derivatives, such as SPAN.<sup>18</sup> The proportion of quinonoid imine (=N-), benzenoid amine (-NH-), and positively charged nitrogen atoms (N<sup>+</sup>), centered at about 398.2, 399.2, and >400 eV,<sup>19</sup> respectively, corresponding to an intrinsic oxidation state and protonation level of PANI, can be quantitatively differentiated in the curve-fitted N1s core level spectrum. The N1s spectra of the protonated and deprotonated SPAN and MWNT/SPAN and the model fits are shown in Figure 4. The optimized parameters such as the fit component peak positions and area percentages are summarized in Table 1.

As shown in Figure 4a, the N 1s spectrum of SPAN can be deconvoluted smoothly into three component peaks centered at 399.3 (-NH-), 400.8 (N<sup>+</sup>), and 401.7 eV (N<sup>+</sup>). The area fractions of these three peaks are 0.49, 0.17, and 0.34, respectively. This leads to the conclusion that all the imine nitrogens have been converted to the positively charged species,

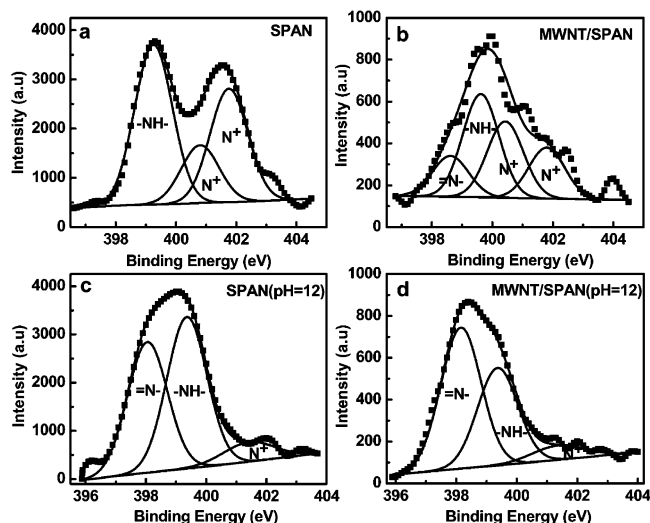


**Figure 4.** N1s core-level spectra of (a) SPAN, (b) MWNT/SPAN, (c) SPAN (pH 12), and (d) MWNT/SPAN (pH 12).

**TABLE 1: N1s Binding Energies (eV) with Their Corresponding Atomic Concentrations of SPAN, MWNT/SPAN, SPAN (pH 12), and MWNT/SPAN (pH 12)**

samples	=N-/N	-NH-/N	N <sup>+</sup> /N
SPAN		399.3 (0.49)	400.8 (0.17) 401.7 (0.34)
MWNT/SPAN	398.6 (0.15)	399.7 (0.38)	400.4 (0.28) 401.8 (0.19)
SPAN (pH 12)	398.1 (0.43)	399.3 (0.49)	401.6 (0.08)
MWNT/SPAN (pH 12)	398.2 (0.55)	399.4 (0.38)	401.4 (0.07)

conforming to the general belief that protonation occurs preferentially at the imine units.<sup>19</sup> However, the N 1s spectrum of the MWNT/SPAN composite gives four component peaks at 398.6 (0.15), 399.7 (0.38), 400.4 (0.28), and 401.8 eV (0.19) (Figure 4b). The binding energies of the latter three peaks are identical with those of SPAN, while that of the first one is due to the quinonoid imine nitrogen (=N-). This result points to an increment of the quinonoid unit in the MWNT/SPAN composite because of the presence of MWNTs.

Moreover, the proportion of quinonoid imine (=N-) and benzenoid amine (-NH-) in the MWNT/SPAN composite or pure SPAN can also be clearly seen in the N1s spectra of their deprotonation states. Upon deprotonation of aqueous MWNT/SPAN and SPAN with NaOH (0.1 M) until the pH is 12, the imine structure can be recovered while the positively charged nitrogen decreases significantly. Thus, the N 1s spectrum of SPAN (pH 12) can be deconvoluted into two major component peaks centered at 398.1 (0.43) and 399.3 eV (0.49) (Figure 4c), which are of about the same area, suggesting that about equal amounts of quinonoid imine and benzenoid amine structure are present in the pure SPAN (pH 12). The slightly lower amount of imine structure observed is probably associated with the presence of a trace amount of positively charged nitrogen. The N 1s spectrum of the MWNT/SPAN composite (pH 12) can also be deconvoluted into two major component peaks centered at 398.2 and 399.4 eV (Figure 4d), but with remarkable difference in area fraction. There are about 55% imine units and 38% amine units in the MWNT/SPAN composite (pH 12). These data reveal that the SPAN in the composite is richer in the quinonoid unit than the pure SPAN. The trend in the XPS spectra may suggest that the interactions between MWNT and SPAN promote and/or stabilize the quinonoid structure, which is in more intimate contact with the graphitic surface of nanotubes.<sup>8a</sup>



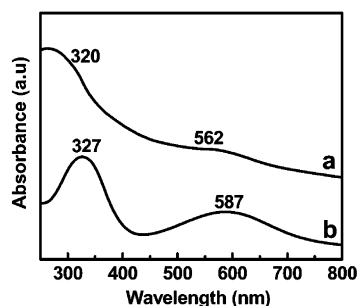


**Figure 5.** UV-vis absorption spectra of (a) MWNT/SPAN and (b) SPAN at pH 12.

To further examine the interaction between SPAN and MWNTs, the UV-vis absorption spectra of the MWNT/SPAN composite (pH 12) and SPAN (pH 12) were measured, as shown in Figure 5. The spectrum of SPAN (pH 12) consists of two major absorption bands. The one around 327 nm is assigned to the  $\pi$ - $\pi^*$  transition and the other one around 587 nm is assigned to a charge-transfer exciton-like transition related to the quinonoid unit, which can be used as a measure of the oxidation state of polyaniline.<sup>19</sup> However, the  $\pi$ - $\pi^*$  transition band shows a blue shift from 327 nm for pure SPAN to 320 nm for the MWNT/SPAN composite (pH 12) and the exciton transition also shows a remarkable blue shift from 587 nm for pure SPAN to 562 nm for the MWNT/SPAN composite (pH 12). The expected blue shifts were also observed in the UV-vis absorption spectrum of the fully oxidized polyaniline (50% quinonoid units) when compared with the half oxidized polyaniline (25% quinonoid units).<sup>19</sup> This situation is mirrored in the XPS spectroscopy that an enhanced number of quinonoid units were formed as a consequence of the in situ polymerization. The quinonoid units were stabilized by the strong  $\pi$ - $\pi$  interaction between MWNTs and SPAN and/or the charge transfer from the polymer chain to MWNTs via the highly reactive imine group as suggested earlier.<sup>8</sup> Besides the enhanced number of quinonoid units existing in the composite, another possibility may be responsible for the blue shift: Since the backbone conformation of polymer was modified due to its interaction with a nanotube,<sup>20</sup> the extent of  $\pi$ -conjugation decreased and the band gap increased, consistent with a blue shift.

Considering both the XPS and UV-vis results, the following hypothesis can be stated: During the in situ polymerization of aniline and MWNTs, more planar quinonoid units are favored so that PANI chains come sufficiently close to the hexagonal lattice of the graphitized MWNT surface and the efficient  $\pi$ - $\pi$  interaction can take place.<sup>10</sup> Such parallel stacking exists as well in the CNT/poly(*p*-phenylenevinylene) (PPV) and the CNT/poly(*m*-phenylenevinylene-*co*-2,5-dioctyloxy-*p*-phenylenevinylene) (PmPV) composite, which significantly increases the overall CNT/polymer interactions.<sup>20</sup> In conclusion, the water-soluble MWNT/SPAN composite combines CNTs and soluble conducting polymer together and allows for their further development of new technological applications in light-emitting diodes, photovoltaic and electrochromic devices, and chemical sensors.<sup>12</sup>

#### 4. Conclusions

Water-soluble SPAN functionalized MWNTs have been prepared via in situ polymerization. The lengths and surface structure of MWNTs were not perturbed by the incorporation of SPAN. On the basis of Raman, XPS, and UV-vis studies, we conclude that MWNTs affect the quinonoid units along the

polymer backbone, which results in a strong interaction between MWNTs and SPAN. The SPAN functionalized MWNTs which are highly dispersible in water hold great promise for various prospective applications.

**Acknowledgment.** This work was supported by National Natural Science Foundation of China (50328204) and the Hi-Tech Research and Development program of China (2002AA327110).

**Supporting Information Available:** Figure S1 showing the TGA curves of MWNTs, MWNT/SPAN, and SPAN. This material is available free of charge via the Internet at <http://pubs.acs.org>.

#### References and Notes

- (1) (a) Iijima, S. *Nature* **1991**, *354*, 56. (b) Baughman, R. H.; Zakhidov, A. A.; de Heer, W. A. *Science* **2002**, *297*, 787.
- (2) (a) Georgakilas, V.; Tagmatarchis, N.; Pantarotto, D.; Bianco, A.; Briand, J. P.; Prato, M. *Chem. Commun.* **2002**, 3050. (b) Zhao, W.; Song, C. H.; Pehrsson, P. E. *J. Am. Chem. Soc.* **2002**, *124*, 12418. (c) Hudson, J. L.; Casavant, M. J.; Tour, J. M. *J. Am. Chem. Soc.* **2004**, *126*, 11158. (d) Hong, C. Y.; You, Y. Z.; Pant, C. Y. *Chem. Mater.* **2005**, *17*, 2247. (e) Sinani, V. A.; Gheith, M. K.; Yaroslavov, A. A.; Rakhnyanskaya, A. A.; Sun, K.; Mamedov, A. A.; Wicksted, J. P.; Kotov, N. A. *J. Am. Chem. Soc.* **2005**, *127*, 3463.
- (3) (a) Hamon, M. A.; Chen, J.; Hu, H.; Chen, Y. S.; Itkis, M. E.; Rao, A. M.; Eklund, P. C.; Haddon, R. C. *Adv. Mater.* **1999**, *11*, 834. (b) Qin, Y. J.; Liu, L. Q.; Shi, J. H.; Wu, W.; Zhang, J.; Guo, Z. X.; Li, Y. F.; Zhu, D. B. *Chem. Mater.* **2003**, *15*, 3256. (c) Kong, H.; Gao, C.; Yan, D. Y. *J. Am. Chem. Soc.* **2004**, *126*, 412. (d) Qin, S. H.; Qin, D. Q.; Ford, W. T.; Resasco, D. E.; Herrera, J. E. *J. Am. Chem. Soc.* **2004**, *126*, 170. (e) Banerjee, S.; Hemraj-Benny, T.; Wong, S. S. *Adv. Mater.* **2005**, *17*, 17. (f) Huang, W. J.; Lin, Y.; Taylor, S.; Gaillard, J.; Rao, A. M.; Sun, Y. P. *Nano Lett.* **2002**, *2*, 231.
- (4) (a) Monthieux, M.; Smith, B. W.; Berteaux, B.; Claye, A.; Fischer, J. E.; Luzzi, D. E. *Carbon* **2001**, *39*, 1251. (b) Garg, A.; Sinnott, S. B. *Chem. Phys. Lett.* **1998**, *295*, 273. (c) Skakalova, V.; Kaiser, A. B.; Dettlaff-Weglikowska, U.; Hrnčarikova, K.; Roth, S. *J. Phys. Chem. B* **2005**, *109*, 7174.
- (5) (a) Islam, M. F.; Rojas, E.; Bergey, D. M.; Johnson, A. T.; Yodh, A. G. *Nano Lett.* **2003**, *3*, 269. (b) Moore, V. C.; Strano, M. S.; Haroz, E. H.; Hauge, R. H.; Smalley, R. E.; Schmidt, J.; Talmon, Y. *Nano Lett.* **2003**, *3*, 1379.
- (6) (a) Dalton, A. B.; Stephan, C.; Coleman, J. N.; McCarthy, B.; Ajayan, P. M.; Lefrant, S.; Bernier, P.; Blau, W. J.; Byrne, H. J. *J. Phys. Chem. B* **2000**, *104*, 10012. (b) Star, A.; Stoddart, J. F.; Steuerman, D.; Diehl, M.; Boukai, A.; Wong, E. W.; Yang, X.; Chung, S. W.; Choi, H.; Heath, J. R. *Angew. Chem., Int. Ed.* **2001**, *40*, 1721. (c) O'Connell, M. J.; Boul, P.; Ericson, L. M.; Huffman, C.; Wang, Y. H.; Haroz, E.; Kuper, C.; Tour, J.; Ausman, K. D.; Smalley, R. E. *Chem. Phys. Lett.* **2001**, *342*, 265. (d) Chen, J.; Liu, H. Y.; Weimer, W. A.; Halls, M. D.; Waldeck, D. H.; Walker, G. C. *J. Am. Chem. Soc.* **2002**, *124*, 9034.
- (7) Shvartzman-Cohen, R.; Nativ-Roth, E.; Baskaran, E.; Levi-Kalishman, Y.; Szleifer, I.; Yerushalmi-Rozen, R. *J. Am. Chem. Soc.* **2004**, *126*, 14850.
- (8) (a) Zengin, H.; Zhou, W. S.; Jin, J. Y.; Czerw, R.; Smith, D. W.; Echegoyen, L.; Carroll, D. L.; Foulger, S. H.; Ballato, J. *Adv. Mater.* **2002**, *14*, 1480. (b) Cochet, M.; Maser, W. K.; Benito, A. M.; Callejas, M. A.; Martinez, M. T.; Benoit, J. M.; Schreiber, J.; Chauvet, O. *Chem. Commun.* **2001**, 1450.
- (9) Valter, B.; Ram, M. K.; Nicolini, C. *Langmuir* **2002**, *18*, 1535.
- (10) Sainz, R.; Benito, A. M.; Martinez, M. T.; Galindo, J. F.; Soares, J.; Baro, A. M.; Corraze, B.; Chauvet, O.; Maser, W. K. *Adv. Mater.* **2005**, *17*, 278.
- (11) (a) Yue, J.; Wang, Z. H.; Cromack, K. R.; Epstein, A. J.; Macdiarmid, A. G. *J. Am. Chem. Soc.* **1991**, *113*, 2665. (b) Chen, S. A.; Hwang, G. W. *Macromolecules* **1996**, *29*, 3950. (c) Wei, X. L.; Wang, Y. Z.; Long, S. M.; Bobeczko, C.; Epstein, A. J. *J. Am. Chem. Soc.* **1996**, *118*, 2545.
- (12) (a) Zhao, B.; Hu, H.; Haddon, R. C. *Adv. Funct. Mater.* **2004**, *14*, 71. (b) Bekyarova, E.; Davis, M.; Burch, T.; Itkis, M. E.; Zhao, B.; Sunshine, S.; Haddon, R. C. *J. Phys. Chem. B* **2004**, *108*, 19717.
- (13) Fan, Y. Y.; Li, F.; Cheng, H. M.; Su, G.; Yu, Y. D.; Shen, Z. H. *J. Mater. Res.* **1998**, *13*, 2342.
- (14) Ito, S.; Murata, K.; Teshima, S.; Aizawa, R.; Asako, Y.; Takahashi, K.; Hoffman, B. M. *Synth. Met.* **1998**, *96*, 161.

- (15) Fernando, K. A. S.; Lin, Y.; Sun, Y. P. *Langmuir* **2004**, *20*, 4777.
- (16) (a) Dresselhaus, M. S.; Dresselhaus, G.; Saito, R.; Jorio, A. *Phys. Rep.* **2005**, *409*, 47. (b) Cochet, M.; Louarn, G.; Quillard, S.; Buisson, J. P.; Lefrant, S. *J. Raman Spectrosc.* **2000**, *31*, 1041.
- (17) Wu, T. M.; Lin, Y. W.; Liao, C. S. *Carbon* **2005**, *43*, 734.

- (18) Wei, X. L.; Fahlman, M.; Epstein, K. J. *Macromolecules* **1999**, *32*, 3114.
- (19) Kang, E. T.; Neoh, K. G.; Tan, K. L. *Prog. Polym. Sci.* **1998**, *23*, 277.
- (20) Yang, M. J.; Koutsos, V.; Zaiser, M. *J. Phys. Chem. B* **2005**, *109*, 10009.